UDC: 46.86’87
https://doi.org/10.59849/2409-4838.2025.3.100

PHASE EQUILIBRIA IN THE $MnSb_4Te_7$-$MnBi_4Te_7$ SYSTEM AND CHARACTERIZATION OF TETRADYMITE-TYPE LAYERED SOLID SOLUTIONS

Sahila Bakir Izzatli[1*], Konul Vaqif Amirmatova[2], Elnur Najaf Orujlu[3]
[1]Baku State University, Baku, Azerbaijan
[2,3]Azerbaijan State Oil and Industry University, Baku, Azerbaijan
*sahile.izzetli@bk.ru
Received: 11.02.2025
Accepted: 03.07.2025

Phase equilibria and structural evolution in the $MnSb_4Te_7$–$MnBi_4Te_7$ system were systematically investigated to understand the formation and stability of tetradymite-type layered solid solutions via X-ray diffraction (XRD), differential thermal analysis (DTA), and scanning electron microscopy (SEM) and its T-x diagram was plotted. XRD analysis confirmed that all synthesized $MnSb_{4-x}Bi_xTe_7$ ($0 \le x \le 4$) alloys crystallize in a single-phase trigonal structure (P-3m1), with no evidence of secondary phases. The gradual substitution of Sb^{3+} by the larger Bi^{3+} ions resulted in a monotonic increase in lattice parameters which determined via Le Bail method, indicating the formation of a continuous solid solution. SEM imaging further confirmed the homogeneous microstructure of the samples, with no visible phase separation or compositional inhomogeneity. The T-x diagram of system is characterized by peritectic transformations. Due to $MnSb_4Te_7$ and $MnBi_4Te_7$ melt incongruently, pseudobinary behavior was observed only in the subsolidus region. The findings highlight the potential of these solid solutions for desired properties, essential for applications in magnetic topological insulators and quantum materials.

Keywords: *phase diagram, tetradymite-type structure, layered chalcogenide, solid solutions,, crystal structure, magnetic topological insulator.*

INTRODUCTION

Tetradymite-type layered metal chalcogenides are a versatile class of materials characterized by their unique layered structures and diverse properties which makes them highly valued for various applications, particularly in thermoelectrics and topological insulators (Tl) [1-4]. Their distinct structural features and the potential for property optimization via chemical modifications position them as a fascinating focus of study novel properties. Recent studies have highlighted that ternary compounds in the *A*Te-Sb(Bi)$_2$Te$_3$ (*A* - Mn, Sn, Ge and Pb) pseudobinary systems exhibit structural features derived from the tetradymite family and possess 3D Tl properties [5-8]. Special attention are focused on manganese antimony and bismuth tellurides since these layered phases show magnetic order and topological insulator properties at the same time [9-16]. The discovery of $MnBi_2Te_4$ as the first intrinsic antiferromagnetic Tl has opened new avenues for research since coexistence of these two features have huge potential applications in spintronics and quantum computing [16].

Despite the promising intrinsic magnetic properties of these Tl, the realization of quantum anomalous Hall effect typically requires extremely low temperatures due to small magnetic gaps and thermal excitation of bulk carriers. Obtention of substitional solid solutions based on $MnBi_2Te_4$ or $MnSb_2Te_4$ not only modifies the electronic structure but also influences the magnetic interactions within the material. Studies have shown that substituting bismuth (Bi) with antimony (Sb) can effectively tune the Fermi level, which is crucial for achieving desired electronic properties. Specifically, the introduction of Sb leads to a transition from n-type to p-type conductivity, thereby altering the magnetic state of the system [17] Similarly, the comparative analysis of the magnetic properties of $MnBi_4Te_7$ and $MnSb_4Te_7$ demonstrates their role as materials that bridge magnetism and topological phenomena.

Although extensive studies in the literature have explored the effects of doping and alloying on these layered phases [18-21], comprehensive phase equilibria data remains scarce, or even entirely absent, despite its critical importance for guiding material synthesis and optimizing functional properties. Given that ternary compounds in the pseudobinary MnTe-$Sb(Bi)_2Te_3$ system form peritectic cascades within a narrow temperature interval [22, 23], a detailed investigation of the phase equilibria in the relevant pseudoternary systems and their vertical sections is essential. This study aims to provide a comprehensive understanding of the phase relationships and solid solution formation in this system, contributing to the rational design of materials with tailored properties for potential applications in spintronics and quantum technologies.

In this work, we investigate the phase relationships in the $MnSb_4Te_7$–$MnBi_4Te_7$ vertical section of the MnTe–Sb_2Te_3–Bi_2Te_3 pseudobinary system and characterize tetradymite-type layered solid solutions via X-ray diffraction (XRD), differential thermal analysis (DTA), and scanning electron microscopy (SEM).

EXPERIMENTAL PART

Starting binary compounds - MnTe, Sb_2Te_3, and Bi_2Te_3 were synthesized using manganese pieces, tin lumps, bismuth shots, and tellurium lumps. Table 1 presents detailed information on the source and purity of all starting materials and synthesized compounds. The weighted pure elemental starting materials were sealed in cleaned silica tubes under a residual pressure of 0.001 Pa and melted in a muffle furnace at 1200, 700, or 650 °C, depending on the binary compounds, then held at these temperatures for 8 hours.

Table 1.

Provenance and purity of the materials used in this study

Chemical	Mass fraction of purity	Source	CAS No	Form	Purity analysis methods
Mn	0.9999	Thermo Scientific Chemicals	7439-96-5	pieces	As stated by the supplier
Sb	0.99999	Thermo Scientific Chemicals	7440-36-0	lump	As stated by the supplier
Bi	0.99999	Thermo Scientific Chemicals	7440-69-9	shots	As stated by the supplier
Te	0.99999	Alfa Aesar	13494-80-9	lump	As stated by the supplier
MnTe	0.999	synthesized by us	12025-39-7	ingot	DTA, XRD
Sb_2Te_3	0.999	synthesized by us	1327-50-0	ingot	DTA, XRD
Bi_2Te_3	0.999	synthesized by us	1304-82-1	ingot	DTA, XRD

$MnSb_{4-x}Bi_xTe_7$ alloys compositions with x=0;0.4;0.8;1.2;1.6 and 2 were synthesized using pre-synthesized binary compound was prepared by the abovementioned method. Synthesis process was carried out at temperatures of 800-1100°C depending on the composition and subsequently quenched in ice water. At the first stage, MnTe-rich alloys were annealed at 700 °C, while the others were treated at 600 °C for 2 weeks. This was followed by a second heat treatment at 500 °C for 6 weeks for all alloys.

In developing the synthesis methodology, we assumed that bulk layered phases obtained via the common fusion method do not reach equilibrium, even after prolonged annealing (2000–3000 hours). This is likely due to the slow interlayer diffusion in van der Waals phases formed under non-equilibrium conditions, such as melt cooling. To prevent large crystal formation, we quenched the alloys from the melt, with subsequent annealing promoting the formation of equilibrium phases.

All equilibrated alloys were examined using DTA, XRD and SEM techniques Phase transformation temperatures were determined by DTA using the LINSEIS HDSC PT1600 system (heating rate: 10 °C/min) and a multichannel DTA device with a TC-08 Thermocouple Data Logger. In the first system, measurements were conducted under a continuous flow of inert helium, while samples were placed in evacuated quartz tubes in the second. To prevent peak overlap, smaller samples (~20 mg) were used. Phase analysis was performed on a Bruker D2 PHASER diffractometer with CuKα radiation, scanning from 2θ = 5° to 75°. The XRD data were analyzed with Match!3 Crystal Impact software, and the PDF-2 and COD databases. Microstructural studies were carried out with a Tescan Vega 3 SBH SEM. Backscattered electron (BSE) imaging was used for detailed analysis. Samples were polished with progressively finer abrasives to achieve a smooth surface and cleaned in an ultrasonic cleaner to remove any residual debris.

RESULTS AND DISCUSSION

A total of seven samples were synthesized and homogenized for this investigation, each corresponding to 20 mol% intervals across the system. General analysis of the XRD patterns confirms that all diffractograms are monophasic, showing no evidence of residual or secondary phases. Representative XRD patterns of selected alloys are shown in Fig. 1. As can be seen, the diffraction peaks of all intermediate compositions qualitatively resemble those of the end-member ternary compounds. However, the substitution of the smaller Sb^{3+} ion with the larger Bi^{3+} ion in the crystal lattice leads to a systematic shift of all peaks toward lower 2θ angles, without introducing additional reflections. Analysis of the diffraction patterns indicates that all peaks can be indexed to a trigonal crystal structure with space group *P*-3m1 (#164). The lattice parameters of the solid solutions were determined from the powder XRD data using the Le Bail refinement method. Fig. 2 presents the final refinement for the alloy with 60 mol% $MnSb_4Te_7$, showing the observed and calculated diffractograms along with the residual line. The refined lattice parameters are listed in Table 2.

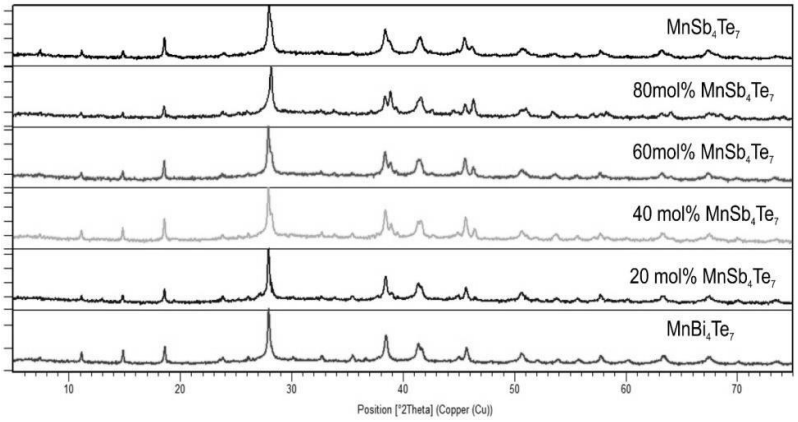

Fig. 1. Powder XRD patterns of $MnSb_{4-x}Bi_xTe_7$ solid solutions

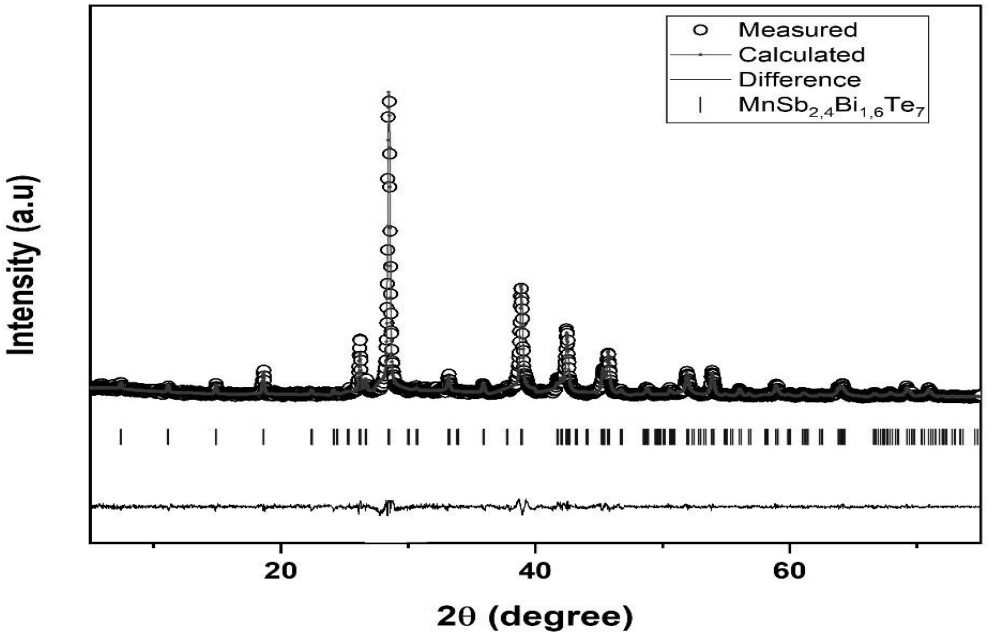

Fig. 2. Full-profile Le-Bail profile for alloy with composition of 60 mol% $MnSb_4Te_7$.

Table 2.

Refined lattice parameters for $MnSb_{4-x}Bi_xTe_7$ solid solutions

Composition, mol%	**Space Group**	**Latice paramaters, Å**		**Ref.**
		a	*c*	
x=0 ($MnSb_4Te_7$)	*P*-3*m*1	4.2513(3)	23.761(4)	[23]
x=0.8	*P*-3*m*1	4,2789(4)	23,776(2)	This work
x=1.6	*P*-3*m*1	4,2989(2)	23,788(6)	This work
x=2.4	*P*-3*m*1	4,3127(5)	23,795(3)	This work
x=3.2	*P*-3*m*1	4,3369(2)	23,809(3)	This work
x=4.0 ($MnBi_4Te_7$)	*P*-3*m*1	4.355(1)	23.815(1)	[22]

The single-phase nature of the synthesized materials was further confirmed by SEM method. SEM images of representative samples demonstrated homogeneous microstructures with no evidence of secondary phases or compositional inhomogeneity. For example, the alloy with the nominal composition $MnSb_{2.4}Bi_{1.6}Te_7$ exhibited uniform contast and morphology as seen in Fig. 3, supporting the XRD findings.

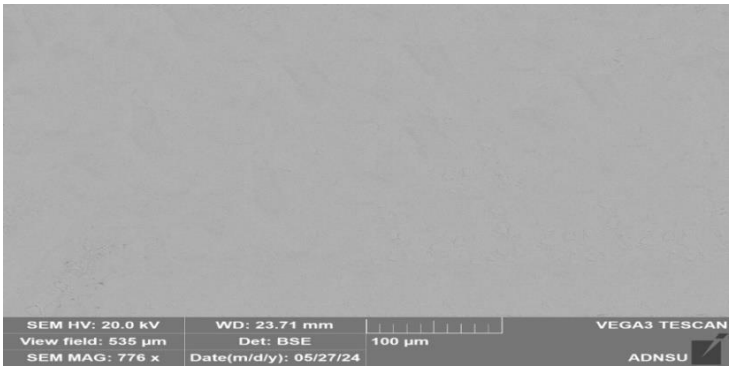

Fig. 3. SEM image of alloy with composition of 60 mol% $MnSb_4Te_7$

The concentration dependence of the lattice parameters for the $MnSb_{4-x}Bi_xTe_7$ solid solution series ($0 < x < 4$) was established based on the values listed in Table 2. As shown in the graph (Fig. 4(a)), a systematic increase in both lattice parameters *a* and *c* is observed with increasing Bi content following Vegard's law. This trend is attributed to the progressive substitution of smaller Sb^{3+} ions by larger Bi^{3+} ions. The continuous and monotonic change in lattice dimensions across the composition range confirms the formation of a complete solid solution without phase separation.

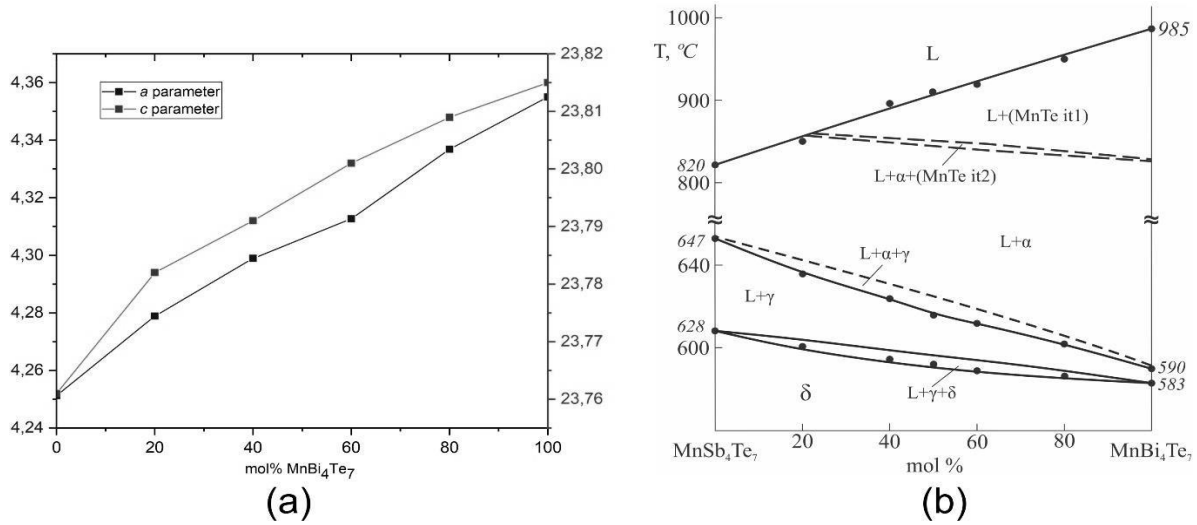

Fig 4. The concentration dependence of the lattice parameters for the $MnSb_{4-x}Bi_xTe_7$ solid solutions (a) and phase diagram of $MnSb_4Te_7$–$MnBi_4Te_7$ system (b). In (b), MnTe it2 and it1 – solid solutions based on different modifications of MnTe; α – a solid solution based on MnTe rt; γ – $MnSb_{2-x}Bi_xTe_4$ solid solutions, δ – $MnSb_{4-x}Bi_xTe_7$ solid solutions

The phase diagram of $MnSb_4Te_7$–$MnBi_4Te_7$ system were plotted using DTA results of homogenized alloys and literature data of MnTe–Sb_2Te_3, as well as MnTe–Bi_2Te_3 pseudobinary systems. The constructed diagram (Fig. 4(b)) shows that the system cannot be considered pseudobinary overall, as both end-member ternary compounds form incongruently. However, pseudobinary behavior is observed in the subsolidus region. As can be seen, solid solutions based on various MnTe structural modifications (rt, it2, it1) are the first to crystallize from the melt. Due to the presence of peritectic cascades involving the ternary compounds at both ends—each occurring within narrow temperature intervals—the monovariant peritectic curves along this system replace one another sequentially. Upon cooling below the liquidus, the initial reaction $L + \alpha \rightleftharpoons \gamma$ takes place. Once the α phase is fully consumed, a twophase area L+γ forms. This is followed by another monovariant reaction, $L + \gamma \rightleftharpoons \delta$, which completes the crystallization process, resulting in a homogeneous δ-phase in the subsolidus range.

CONCLUSION

A comprehensive investigation of the $MnSb_4Te_7$–$MnBi_4Te_7$ system has been conducted to establish the phase equilibria and structural behavior of tetradymite-type layered solid solutions. XRD analysis confirmed that all synthesized $MnSb_{4-x}Bi_xTe_7$ compositions ($0 \leq x \leq 4$) form a continuous solid solution with a trigonal *P*-3*m1* structure, obeying Vegard's law. Lattice parameters were refined using Le Bail method. SEM imaging verified the microstructural homogeneity of the alloys, while DTA results enabled the construction of phase diagram. The system is characterized by peritectic transformations and incongruent melting at both ends, with pseudobinary behavior observed in the subsolidus region. The crystallographic and thermal data reported here offer essential insights for the targeted development and tuning of magnetic topological materials based on Mn-containing layered chalcogenides.

REFERENCES

1. Wang L.L., Johnson D.D. Ternary tetradymite compounds as topological insulators // Phys. Rev. B, - 2011. - v.83 (24), - p. 241309.
2. Rakshit M., Jana D., Banerjee D. General strategies to improve thermoelectric performance with an emphasis on tin and germanium chalcogenides as thermoelectric materials // J. Mater. Chem. A, - 2022. - v.10, - p. 6872–6926.
3. Goldsmid H.J. Bismuth telluride and its alloys as materials for thermoelectric generation // Materials, - 2014. - v.7, - p. 2577–2592.
4. Heremans J., Cava R., Samarth N. Tetradymites as thermoelectrics and topological insulators // Nat. Rev. Mater., - 2017. - v.2, - p. 17049.
5. Nurmamat M., Okamoto K., Zhu S., Menshchikova T.V., Rusinov I.P., Korostelev V. O., Miyamoto K., Okuda T., Miyashita T., Wang X., IshidaY., Sumida K., Schwier E.F., Ye M., Aliev Z.S., Babanly M.B., Amiraslanov I.R., Chulkov E.V., Kokh K. A., Tereshchenko O.E., Shimada K., Shin S., Kimura A. Topologically non-trivial phase-change compound $GeSb_2Te_4$ // ACS Nano, - 2020. - v.14 (7), - p. 9059-9065**.**
6. Eremeev S.V., De Luca O., Sheverdyaeva P.M., Ferrari L., Matetskiy A.V., Di Santo G., Petaccia L., Crovara C., Caruso T., Papagno M., Agostino R.G., Aliev Z.S., Moras P., Carbone C., Chulkov E.V., Pacilè D. Energy-overlap of the Dirac surface state with bulk bands in $SnBi_2Te_4$ // Phys. Rev. Materials, - 2023. - v.7, - p. 014203.
7. Wang L.-L. Highly tunable band inversion in AB_2X_4 (A=Ge, Sn, Pb; B=As, Sb, Bi; X=Se, Te) compounds // Phys. Rev. Materials, - 2022, - v.6, - p. 094201.
8. Zhou W., Li B., Shen Y., Feng J.J., Xu C.Q., Guo H.T., He Z., Qian B., Zhu Z., Xu X. Multiple superconducting phases driven by pressure in the topological insulator $GeSb_4Te_7$ // Phys. Rev. B, - 2023. - v.108, - p. 184504.
9. Eremeev S.V., Otrokov M.M., Ernst A., Chulkov E.V. Magnetic ordering and topology in $Mn_2Bi_2Te_5$ and $Mn_2Sb_2Te_5$ van der Waals materials // Phys. Rev. B, - 2022, - v.105, - p. 195105.
10. Yan J.-Q., Zhang Q., Heitmann T., Huang Z., Chen K.Y., Cheng J.-G., Wu W., Vaknin D., Sales B.C., McQueeney R.J. Crystal growth and magnetic structure of $MnBi_2Te_4$ // Phys. Rev. Materials, - 2019. - v.3, - p. 064202.
11. Li Y., Jiang Z., Li J., Xu S., Duan W. Magnetic anisotropy of the two-dimensional ferromagnetic insulator $MnBi_2Te_4$ // Phys. Rev. B, - 2019. - v. 100, - p. 134438.
12. Ren Y., Ke S., Lou W.-K., Chang K. Quantum phase transitions driven by sliding in bilayer MnBi2Te4, Phys. Rev. B, - 2022. -v.106, - p. 235302 .
13. Yang X., Pan J., He X., Chu D. Critical behavior, magnetic phase diagram, and magnetic entropy change of $MnSb_2Te_4$ // Phys. Rev. B, - 2024. - v.109, -p. 094408.

14. Pei C., Xi M., Wang Q., Shi W., Wu J., Gao L., Zhao Y., Tian S., Cao W., Li C., Zhang M., Zhu S., Chen Y., Lei H., Qi Y. Pressure-induced superconductivity in magnetic topological insulator candidate $MnSb_4Te_7$ // Phys. Rev. Materials, - 2022. - v.6, - p. L101801.
15. Yan J.-Q., Liu Y.H., Parker D.S., Wu Y., Aczel A.A., Matsuda M., McGuire M.A., Sales B.C. A-type antiferromagnetic order in $MnBi_4Te_7$ and $MnBi_6Te_{10}$ single crystals // Phys. Rev. Materials, - 2020. - v.4, - p. 054202.
16. Hu C., Ding L., Gordon K.N., Ghosh B., Tien H.-J., Li H., Linn A.G., Lien S.-W., Huang C.-Y., Mackey S., Liu J., Reddy P.V.S., Singh B., Agarwal A., Bansil A., Song M., Li D., Xu S.-Y., Lin H., Cao H., Chang T.-R., Dessau D., Ni N. Realization of an intrinsic ferromagnetic topological state in $MnBi_8Te_{13}$ // Sci. Adv., - 2020. - v.6.
17. Yan J.-Q., Okamoto S., McGuire M.A., May A.F., McQueeney R.J., Sales B.C. Evolution of structural, magnetic, and transport properties in $MnBi_{2-x}Sb_xTe_4$ // Phys. Rev. B, - 2019. -v.100, - p.104409.
18. Hu C., Lien S.-W., Feng E., Mackey S., Tien H.-J., Mazin I.I., Cao H., Chang T.-R. Ni N. Tuning magnetism and band topology through antisite defects in Sb-doped $MnBi_4Te_7$ // Phys. Rev. B, - 2021. - v.104, - p. 054422
19. Mukherjee S., Anjan Kumar N. M., Manna S., Nath S.G., Gopal R.K., Mitra C., Kamaraju N. Magnetic order influenced phonon and electron dynamics in $MnBi_2Te_4$ and Sb-doped $MnBi_2Te_4$ investigated by terahertz time-domain spectroscopy // Phys. Rev. B, - 2024. -v.110, - p. 195401.
20. Shikin A.M., Estyunin D.A., Zaitsev N.L., Estyunina T.P., Eryzhenkov A.V., Rybkin A.G., Kokh K.A., Tereshchenko O.E., Iwata T., Kuroda K., Miyamoto K., Okuda T., Shimada K., Tarasov A.V. Spin texture tunability in $Mn_{1-x}Ge_xBi_2Te_4$ through varying Ge concentration // Phys. Rev. B, -2025. -v.111, - p.115158.
21. Tarasov A.V., Estyunin D.A., Rybkin A.G., Frolov A.S., Sergeev A.I., Eryzhenkov A.V., Anferova V.V., Estyunina T.P., Glazkova D.A., Kokh K.A., Golyashov V.A., Tereshchenko O.E., Ideta S., Miyai Y., Kumar Y., Shimada K., Shikin A.M. Probing the interaction between topological and Rashba-like surface states in $MnBi_2Te_4$ through Sn doping // Phys. Rev. B, - 2025. - v.111, - p.165115
22. Aliev Z. S., Amiraslanov I. R., Nasonova D. I., Shevelkov A. V., Abdullayev N. A., Jahangirli Z. A., Orujlu E. N., Otrokov M. M., Mamedov N. T., Babanly M. B., Chulkov E. V. Novel ternary layered manganese bismuth tellurides of the $MnTe$-Bi_2Te_3 system: synthesis and crystal structure // Journal of Alloys and Compounds, - 2019. - v.789, -p 443–450.
23. Orujlu E. N., Aliev Z. S., Amiraslanov I. R., Babanly M. B. Phase Equilibria of the $MnTe$-Sb_2Te_3 System and Synthesis of Novel Ternary Layered Compound – $MnSb_4Te_7$. // Physics and Chemistry of Solid State, - 2021. - v.22, - p. 39 – 44.

$MnSb_4Te_7$-$MnBi_4Te_7$ SİSTEMİNDƏ FAZA TARAZLIQLARININ TƏDQİQİ VƏ TETRADİMİTƏBƏNZƏR LAYLI QURULUŞLU BƏRK MƏHLULLARIN XARAKTERİZƏ EDİLMƏSİ

S.B. İzzətli, K.V. Əmirmətova, E.N. Oruclu

Tetradimitəbənzər laylı quruluşlu bərk məhlulların əmələ gəlməsi və stabilliyinin tədiqi üçün $MnSb_4Te_7$–$MnBi_4Te_7$ sistemində faza tarazlıqları və quruluş dəyişiklikləri rentgenfaza, differensial termiki analiz və skanedici elektron mikroskopu ilə öyrənilmişdir və sistemin T-x diaqramı qurulmuşdur. RFA nəticələri sistemdə $MnSb_{4-x}Bi_xTe_7$ ($0 \leq x \leq 4$) formuluna malik triqonal quruluşda (P-3m1) kristallaşan bircins bərk məhlulların əmələ gəlməsini təsdiqləyir. Le-Bail analizi nəticələri göstərir ki, bərk məhlullarda kristal qəfəsdə Sb^{3+} ionunun daha böyük Bi^{3+}ilə əvəz olunmasına görə qəfəs parametrləri xətti qanunla artır. SEM nəticələri ərintilərin tərkibinin bircins olmasını təsdiqləyir. Sistemin faza diaqramı peritektik keçidlərlə xarakteziə olunur. $MnSb_4Te_7$ və

$MnBi_4Te_7$ birləşmələri inkonqruyent əridikləri üçün, sistem yalnız subsolidusda kvazibinardır. Aşkar olunan nəticələr bu bərk məhlulların maqnetik topoloji izolyatorlar və kvant materialları kimi tətbiqlər üçün lazım olan xüsusiyyətlərə malik olduğunu vurğulayır.

Açar sözlər: *faza diaqramı, tetradimitəbənzər quruluş, laylı xalkogenidlər, bərk məhlullar, kristal quruluş, maqnetik topoloji izolyatorlar.*

ФАЗОВЫЕ РАВНОВЕСИЯ В СИСТЕМЕ $MnSb_4Te_7$-$MnBi_4Te_7$ И ХАРАКТЕРИСТИКА СЛОИСТЫХ ТВЕРДЫХ РАСТВОРОВ ТЕТРАДИМИТОВОГО ТИПА

С.Б. Иззатли, К.В. Амирметова, Э.Н. Оруджлу

Фазовые равновесия и структурная эволюция в системе $MnSb_4Te_7$–$MnBi_4Te_7$ были систематически исследованы для понимания формирования и стабильности слоистых твердых растворов типа тетрадимита с помощью рентгеновской дифракции, дифференциального термического анализа и сканирующей электронной микроскопии. Была построена T-x диаграмма системы. Анализ РФА подтвердил, что все синтезированные сплавы $MnSb_{4-x}Bi_xTe_7$ ($0 \leq x \leq 4$) кристаллизуются в однофазной тригональной структуре (P-3m1), без признаков вторичных фаз. Постепенная замена Sb^{3+} более крупными ионами Bi^{3+} привела к монотонному увеличению параметров решетки, что было определено методом Ли Бэйла, что указывает на образование непрерывного твердофазного раствора. СЭМ-изображения дополнительно подтвердили однородную микроструктуру образцов без видимого разделения фаз или композиционной неоднородности. Диаграмма T-x системы характеризуется перитектическими превращениями. Поскольку $MnSb_4Te_7$ и $MnBi_4Te_7$ плавятся неконгруэнтно, псевдобинарное поведение наблюдается только в подсолидусной области. Полученные результаты подчеркивают потенциал этих твердых растворов для достижения желаемых свойств, необходимых для применения в магнитных топологических изоляторах и квантовых материалах.

Ключевые слова: *фазовая диаграмма, структура типа тетрадимита, слоистый халькогенид, твердые растворы, кристаллическая структура, магнитный топологический изолятор.*